doi: 10.56761/EFRE2022.N1-O-038601

The mechanical response of titanium alloys to dynamic impacts in a wide temperature range

V.A. Skripnyak[*], *V.V. Skripnyak, K.V. Iohim, E.G. Skripnyak*

National Research Tomsk State University, Russian Federation
[*]*skrp2006@yandex.ru*

Abstract. The paper presents the results of numerical simulation mechanical behavior hexagonal close packed titanium alloys under dynamic loadings in a temperature range up to temperature of alpha-beta phase transitions. The model of a damaged medium was proposed to describe the response of titanium alloys VT1-0, VT5-1, VT6 at high strain rates and at elevated temperatures. The model takes into account the change in the contributions to the flow stress from the mechanisms of twinning and dislocation slip in the considered subgroup of hexagonal close packed alloys. Thus, it was possible to increase the accuracy of predicting of dynamic fracture of titanium under tensile loads, including the spall fracture. The model allows describing both spall fracture and tensile fracture at high strain rates under conditions of a complex stress state. The constitutive equation takes into account the change in flow stress in wide range of a cumulative plastic strain, a homologous temperature, and the logarithm of the normalized equivalent strain rate. The influence of the damage parameter, the stress state triaxiality parameter on the flow stress is taken into account by the Gurson–Tvergaard's model. These inelastic strains occur during repeated loading of the alloy in reflected loading and unloading waves.

Keywords: fracture titanium alloys, dynamic loading, high strain rate, elevated temperature

1. Introduction

Titanium alloys are used for the production of critical structural elements of aviation, space technology, submarines and surface ships, automotive industry, nuclear power, medical instruments and implants, tools for material processing in various industries [1]. Polycrystalline alpha titanium alloys belong to the isomechanical group of alloys with a hexagonal close-packed lattice (HCP). Interest in the mechanical properties of this class of titanium alloys has been steadily increasing in the last decade due to their expanded use in additive technologies for creating structures using 3D printing methods (selective laser melting – SLM) as well as the improvement of technologies for creating 3D titanium structures using welding [2–4]. However, knowledge of the mechanical response of alpha titanium alloys to dynamic loadings and at elevated or low temperatures is still limited by insufficiency of experimental data.

Microstructural studies of specimens subjected to impact loading have made it possible to propose an interpretation of the physical mechanisms of tensile fracture at high strain rates. The results of studies of macro damages using x-ray tomography (XRT) made it possible to reconstruct the distribution of defects in the spall fracture zone [5–7]. It was established that the interaction of rarefaction waves resulting from the reflection of stress waves from the surfaces of loaded bodies causes the local volumes of the body are subjected to tensile stresses. These tensile stresses are one of the main causes of spall fracture and fragmentation [8]. The available experimental data obtained for alpha titanium alloys indicate that the ductile fracture is a result of micro mechanisms of the nucleation, growth and coalescence of micro damages occurs at high strain rates and the homological temperatures from 0.1 to 0.595. The homological temperature of ~ 0.595 corresponds to temperature of $\alpha \rightarrow \beta$ phase transition. Since the process of formation of micro voids takes place in time, the mechanical behavior of titanium alloys under tension depends on the duration and magnitude of tensile stresses. A number of models within the framework of the continuous and discrete-continuous approaches have been proposed to describe the mechanical behavior of titanium alloys under intense dynamic influences [9–14]. Studies of spall strength have shown that spall strength increases with increasing pulse duration [15].

Modern experimental techniques of laser interferometry for recording the motion of the back surface of flat samples loaded with shock pulses, registration of damage in the region of high-speed tension using synchrotron radiation sources made it possible to establish that the process of dynamic fracture has multi stages [5–15].

The model of a damaged medium was proposed to describe the dynamic fracture of titanium alloys VT1-0, VT5-1, VT6, which allows one to describe both spall fracture and tensile fracture at high strain rates under conditions of a complex stress state [14, 16–18].

Zerilli and Armstrong proposed various constitutive equations based on the dislocation kinetics of plastic flow and taking into account the difference in the regularities of strain hardening, thermal softening, and flow stress rate sensitivity for titanium alloys [9]. Nemat-Nasser et al. showed that, in order to adequately describe the high rate deformation of CP-Ti, it is necessary to take into account, in addition to the motion of dislocations, the contributions of twins [11]. Gao et al. proposed the modification of a constitutive model for Ti-6Al-4V in a wide range of strain rates and temperatures, in comparison with the constitutive equations of the Johnson-Cook and Armstrong Zerilli models [12]. Song et al analyzed the experimental data of Nemat-Nasser and proposed a model to describe the influence of the dynamic strain aging- on the mechanical behavior of titanium alloys in a wide range of strain rates and temperatures up to 1000 K [13].

This work aimed to study the processes of deformation, damage and ductile fracture of alpha titanium alloys under dynamic influences. Based on the generalization of experimental data, a version of the model is proposed that allows to adequately describing the mechanical behavior titanium alloys.

2. Constitutive equation for alpha titanium alloys

Boundary problems describing a mechanical response of titanium constructional elements includes initial and boundaries conditions, and system of conservation equations of continual medium, kinematic relations, constitutive relations, equation of states, model of damage and fracture of material as continuum medium. The most difficult problem is describing the mechanical behavior of HCP titanium alloys in a wide range of strain rates and elevated temperature.

In this work, a constitutive equation (1)–(4) was used to describe the mechanical behavior of titanium alloys with a hexagonal close-packed crystal lattice within the framework of the mechanics of damaged media approach.

$$\sigma_{ij} = -p\delta_{ij} + S_{ij}, \tag{1}$$

$$\begin{cases} p = p^{(m)}\,\Psi_1(f)\ ,\ S_{ij} = S_{ij}^{(m)}\Psi_2(f), \\ p^{(m)} = p_x^{(m)}(\rho) + \Gamma(\rho)\rho E_T, \\ E = E_c + E_T, \\ p_x^{(m)} = 3B_0 \cdot (\rho_0/\rho)^{-2/3} \cdot (1-(\rho_0/\rho)^{1/3}) \cdot \exp[\frac{3}{2}(B_1-1)\cdot(1-(\rho_0/\rho)^{1/3})]\ \ if\ p^{(m)} \geq 0, \\ p_x^{(m)} = B_0(1-\rho_0/\rho)\ if\ \ p^{(m)} < 0, \\ E_{\mathrm{T}} = C_p^{(m)}T, \end{cases} \tag{2}$$

$$\begin{cases} DS_{ij}^{(m)} / Dt = 2\mu(\dot{\varepsilon}_{ij}^{e} - \delta_{ij}\dot{\varepsilon}_{kk}^{e} / 3), \\ DS_{ij}^{(m)} / Dt = dS_{ij}^{(m)} / dt - S_{ik}^{(m)}\dot{\omega}_{jk} - S_{jk}^{(m)}\dot{\omega}_{ik}; \\ \dot{\varepsilon}_{ij} = \dot{\varepsilon}_{ij}^{e} + \dot{\varepsilon}_{ij}^{p}, \ \dot{\varepsilon}_{ij}^{p} = \dot{e}_{ij}^{p} + \delta_{ij}\dot{\varepsilon}_{kk}^{p} / 3. \end{cases} \quad (3)$$

$$\dot{e}_{ij}^{p} = \lambda\partial\Phi / \partial\sigma_{ij}, \ \dot{\varepsilon}_{kk}^{p} = \dot{f}_{growth} / (1 - f).$$

$$\Phi = (\sigma_{eq}{}^{2} / \sigma_{s}{}^{2}) + 2q_1 f^{*}\cosh(-q_2\, p / 2\sigma_s) - 1 - q_3(f^{*})^{2}, \quad (4)$$

where σ_{ij} is the component of stress tensor, p is the pressure, S_{ij} is the deviator of stress tensor components, (m) is superscript indicating that the parameter corresponds to the condensed phase of the damaged medium, (0) – subscript indicating that the parameter corresponds to the initial state, ρ is the mass density, u_i is the components of the particle velocity vector, x_i is Cartesian coordinates, i = 1, 2, 3, E is the specific internal energy, E_T is the thermal part of the internal energy, E_C is the "cold" part of the internal energy, T is the temperature, $\dot{\varepsilon}_{ij}, \dot{\omega}_{ij}$, are the components of strain rate tensor and the bending–torsion tensor, $\psi_i(f)$ functions established a relation between the effective stresses of the damaged medium and the stresses in the condensed phase, Γ is the Grüneisen coefficient, ρ_0 is the initial mass density of the condensed phase of the alloy, γ_R, ρ_R, n, B_0, B_1 are the material's constants, C_p is the specific heat capacity, $D(\cdot)/Dt$ is the Jaumann's derivative, μ is the shear modulus, $\dot{f}_{growth}$ is the damage growth rate, f is the damage parameter, σ_s is the yield stress, σ_{eq} is equivalent stress, p is the pressure, q_1, q_2, and q_3 are damage model parameters, and f^* is the specific volume of damages, λ is the plastic multiplier derived from the consistency condition $\Phi = 0$, and Φ is the plastic potential of damaged medium in the form of Gurson-Tvergaard.

The temperature rise due to the dissipative effect of plastic flow was calculated by the equation (5):

$$T = T_0 + \int_0^{\varepsilon_{eq}^{p}} (\beta / \rho C_p)\sigma_{eq} d\varepsilon_{eq}^{p}, \quad (5)$$

where T_0 is the initial temperature, ρ is the mass density, and $\beta \sim 0.9$ is the parameter representing a fraction of plastic work converted into heat, σ_{eq} is the equivalent stress, ε^{p}_{eq} is the equivalent plastic strain.

The specific heat capacity C_p of titanium alloys changes under dynamic compression. The accuracy of predicting pressure using Eq. (2), and the temperature rise using equation (5) depends on the adequacy of the description of the dependence of specific heat on temperature.

Specific heat capacity C_p and the shear modulus μ for HCP titanium alloys were calculated using phenomenological relations (6) and (7) in the temperature range of existence of a stable alpha phase of the alloys [19].

$$C_p(T) = C_{p0} + C_{p1}T + C_{p2}T^{2}, \ T \le T_{pt}, \quad (6)$$

where C_p is the specific heat capacity, $T_{\alpha\to\beta}$ is the temperature of alpha–beta phase transition, C_{p0}, C_{p1}, C_{p2} are material constants.

Coefficients of Eq. (6) for several alpha titanium alloys are shown in Table 1.

Table 1. Specific heat capacity of several alpha titanium alloys.

Alloy	C_{p0}, J/kg K	C_{p1}, J/kg K^2	C_{p2}, J/kg K^3	$T_{\alpha\beta}$, K at the pressure of 10^5 Pa	T_m, K
CP Ti	522.61	0.210	0	1155–1252	1941
Ti-6Al-4V	493.6	0.0737	0.000195	1268±20	1933
Ti-5Al-2.5Sn	458	0.35	-0.0001929	1153–1311	1863

Estimates of the values of the shear modulus $\mu(T, \rho)$ in wide ranges of temperature and pressure were obtained using the relation (7) [20]:

$$\mu(T,\rho) = \mu_0\left[1+\mu_1 p(\rho_0/\rho)^{1/3} - \mu_2(T-295)\right], \quad (7)$$

where μ_0, μ_1, μ_2 are material constants, T is temperature, p is pressure, ρ_0/ρ is specific volume of alloy.

The change in mass density during heating or cooling of HCP titanium alloys at the pressure of 105 Pa is determined by the formula (8):

$$\rho(T) = \rho_0\left(1-\alpha_v(T-295)\right), \quad (8)$$

where α_v is the volume coefficient of thermal expansion, ρ_0 is the mass density at normal condition; α_l is the coefficient of thermal expansion (CTE).

In alpha titanium alloys, α_v can be determined as isotropic or anisotropic [21, 22]. The volume thermal expansion coefficient αv is approximately equal to ~$3\alpha_l$. The mass density ρ at the temperature T is determined by formula:

$$\rho(T) \approx \rho_0\left(1-3\alpha_l(T-295)\right), \quad (9)$$

where ρ_0 is the initial mass density.

The coefficients of Eqs. (2), (6), (7), and (9) for several alpha titanium alloys showed in Table 2 [14].

Table 2. Coefficients for several alpha titanium alloys

Alloys	B_0, GPa	B’	Γ	μ_0, GPa	μ_1, TPa^{-1}	$-\mu_2$, K^{-1}	Temperature range, K	ρ_0, g/cm^3 at the normal condition	CTE, 10^{-6}, K^{-1}
CP Ti	141.53±11	4.0	1.09	41.45	11.5	0.0006649	150–1155	4.54	8.4–8.6
Ti-5Al-2.5Sn	107±2	4.0	1.09	42.66	11.5	0.000662	300–1313	4.48	9.4–9.7
Ti-6Al-4V	154.018	5.4468	1.09	43.4	11.5	0.00062	300–1268	4.429	8.7–9.1

Sound velocities of isotropic materials can be calculated by relations (10):

$$C_s = (\mu/\rho)^{1/2},\ C_b = (B/\rho)^{1/2},\ C_L = \left(C_b^2 + 4C_s^2/3\right)^{1/2}, \quad (10)$$

where C_s, C_b, C_L are the shear, the bulk, and the longitudinal sound velocities, μ is the shear modulus, B is the bulk modulus, ρ is the mass density.

The plastic flow stress is described by Eq. (11). It is proposed to represent the macroscopic plastic flow stress as the sum of the contributions of the stresses required to overcome the resistance to dislocation slip, resistance to twinning, and stresses from the inhomogeneity of the phase composition of the alloy.

$$\begin{cases} \sigma_S = \sigma_0 \dfrac{\mu(T,\rho)}{\mu(295\,K,\rho_0)} + \\ +\left(C_0\left(\varepsilon_{eq}^p\right)^{1/2} + k_{hp}^{disl} d_g^{-1/2}\right)\exp\left(-\alpha_0 T\right)\exp\left(\alpha_1 T \ln\left(1+\dfrac{\dot{\varepsilon}_{eq}^p}{\dot{\varepsilon}_{disl0}^p}\right)\right) + \\ +\left(A_0\varepsilon_{eq}^p + k_{hp}^{tw} d_g^{-1/2}\right)\exp\left(-\beta_0 T\right)\exp\left(\beta_1 T \ln\left(1+\dfrac{\dot{\varepsilon}_{eq}^p}{\dot{\varepsilon}_{tw0}^p}\right)\right)\exp\left(-(2\pi)^{1/2}|N|\right), \\ A_0(\sigma_1 \ge 0) \ne A_0(\sigma_1 < 0); \\ N = \sum_k \Delta N_k\ , \\ \Delta N_k = \operatorname{sgn}(S_2)\dfrac{\Delta\varepsilon^p{}_k}{n_1 \exp\left(-n_2 \ln\left(\dfrac{\dot{\varepsilon}_{eq}^p}{\dot{\varepsilon}_0^p}\right)\right)}\dfrac{\mu(T,\rho)}{\mu(295\,K,\rho_0)}\exp\left[(2\pi)^{1/2}\cdot\min\left\{\operatorname{sgn}(-S_2)\cdot N, 0\right\}\right], \end{cases} \tag{11}$$

where σ_0 is material parameter depending on the phase composition of the material, μ(T, ρ) is the shear modulus, d_g is the grain size, k_{hp}^{disl}, C_0, α_0, α_1 are material parameters, $\dot{\varepsilon}_0^p$ is parameter normalizing the plastic strain rate, ε_{eq}^p is the equivalent plastic strain, k_{hp}^{tw}, A_0, β_0, β_1 are material parameters, N is a phenomenological parameter that takes into account the possibility of de twinning when the shear stress sign changes, S_2 is the second principal stress, n_1, n_2 are constant of material, $\Delta\varepsilon_k^p$ is the increment of equivalent plastic strain during unloading.

The coefficients of Eq. (11) for several alpha titanium alloys showed in Table 3 [14].

Table 3. Parameters of constitutive equation for several alpha titanium alloys

Alloy	C_0, GPa	k_{hp}^{disl}, GPa μm$^{1/2}$	α_0, K^{-1}	α_1, K^{-1}	$\dot{\varepsilon}_{disl0}^p$, s^{-1}	A_0, GPa	k_{hp}^{tw}, GPa μm$^{1/2}$	β_0, K^{-1}	β_1, K^{-1}	$\dot{\varepsilon}_{tw0}^p$, s^{-1}
CP Ti	0.4	0.269	0.00224	0.00275	10^3	1.85	0.18	0.0002	0.000973	10^3
Ti-6Al-4V	1.05	0. 269	0.0022	0.00205	10^3	1.85	0.4297	0.0002	0.001809	10^3
Ti-5Al-2.5Sn	0.665	0.628	0.0224	0.002	10^3	1.5	0.628	0.0002	0.00222	10^3

Ductile fracture of alpha titanium alloys is the result of the damage nucleation and growth at the mesoscopic level. The damage evolution in alpha titanium alloys under dynamic loadings occurs due to the exhaustion of the possibility of local accommodation of plastic deformation in the bands of localized shear or in the zone from the intersection. The modified damage model (12) was proposed for dynamic fracture prediction [16, 23, 24].

$$\begin{cases} \dot{f} = \dot{f}_{nucl} + \dot{f}_{growth}; \\ \dot{f}_{nucl} = \dot{f}_{nucl}^{(strain)} + \dot{f}_{nucl}^{(stress)}; \\ \dot{f}_{nucl}^{(strain)} = \left[f_N \Big/ \left(s_N\sqrt{2\pi}\right)\right]\exp\left\{-0.5\left[\left(\varepsilon_{eq}^p - \varepsilon_N\right)\Big/ s_N\right]^2\right\}, \\ \dot{f}_{nucl}^{(stress)} = C_1\dot{\sigma}_{eq} + C_2\,\dot{\sigma}_{kk} \quad if \quad \sigma_{kk} > 0\ (tension\ in\ the\ spall\ zone); \\ \dot{f}_{growth} = (1-f)\,\dot{\varepsilon}_{kk}^p, \end{cases} \tag{12}$$

where f are the damage parameters, C_1, C_2, f_N are model parameters, ε_N and s_N are the average nucleation strain and the standard deviation respectively.

The specific volume of damages f^* was calculated by relation (13).

$$f^* = f \cdot H(f_c - f) + \left[f_c + \left(\overline{f}_F - f_c \right) / \left(f_F - f_c \right) \right] \cdot H(f - f_c), \tag{13}$$

where f is damage parameter, $H(.)$ is the Heaviside function, $\overline{f}_F = (q_1 + (q_1^2 - q_3)^{1/2}) / q_3$, f_c is failure parameter.

The fracture criterion (14) was used in the calculations.

$$f^* \geq 0.3 . \tag{14}$$

Parameters of Eq. (12) and Eq. (13) are shown in Table 4.

Table 4. Parameters of the fracture model for several alpha titanium alloys

Alloys	q_1	q_2	q_3	f_0	f_N	fc	f_F	ε_N	s_N
CP Ti	1.5	1	1.6	0.001	0.002	0.035	0.12	0.3	0.005
Ti-5Al-2.5Sn	1.	0.7	1.	0 .003	0.1156	0.117	0.260	0.11	0.005
Ti-6Al-4V	1.5	1	1.5	0.001	0.04	0.03	0.04	0.05	0.1

The proposed constitutive equation and damage model include material coefficients whose numerical values for alloys can be estimated using a set of experimental data from independent experiments on the laws of deformation and fracture of alloys in a wide range of deformation rates and temperatures.

The model was used for numerical simulation of tension of flat specimens of titanium alloys with strain rates from 0.1, to 1000 s^{-1} and also processes of high velocity flat impacts of plates. The LS DYNA solver (ANSYS WB 15.2, ANSYS, Inc., and Canonsburg, PA) was used for numerical solution of boundary value problems using the proposed constitutive equation and fracture model. The constitutive relations have been implemented in the LS-DYNA explicit solver by writing a FORTRAN user-subroutine. A grid with eight-node linear blocks and reduced integration along with hourglass control was used for numerical simulation.

3. Results and discussion

Fig.1a shows the dependences of normalized shear modulus versus the homologous temperature T/T_m for several alpha titanium alloys. The calculated longitudinal sound velocity of some HCP alloys versus temperature is shown in Fig.1b. As the temperature rises to the temperature T_{pt} of $\alpha \rightarrow \beta$ phase transition, the value of the longitudinal speed of sound in titanium alloys decreases by more than 15%.

The calculated stress-strain diagrams obtained under uniaxial high-velocity tension of Ti-5Al-2.5Sn and Ti-6Al-4V alloys at various initial temperatures in comparison with experimental data are shown in Fig.1b. At the room temperature and at elevated temperatures, the strain hardening of the alloy at high rate strain and strain is mainly determined by the contributions from dislocation slip. The simulation results confirmed that strain hardening can be considered as a result of the simultaneous action of thermally activated dislocation mechanisms of plasticity and twinning, which weakly depends on temperature.

The computational stress-strain diagrams obtained when simulating uniaxial high-velocity tension of Ti-5Al-2.5Sn flat specimens at initial temperatures from 298 K to 873 K in comparison with experimental data [16, 25, 26] are shown in Fig.1c. Stress-strain curves under tension of Ti-6Al-4V alloy samples at initial temperatures from 298 K to 1373 K in comparison with

experimental data [27] are shown in Fig.1d. The calculation results obtained using the proposed constitutive equation is consistent with experimental data on the deformation of alpha titanium alloys under quasi-static and high-speed loading in a wide temperature range. This confirms the assumptions made when constructing the constitutive equation. Thus, at room temperature and at elevated temperatures, the strain hardening of the alloy at high rate strain and strain is mainly determined by the contributions from dislocation slip.

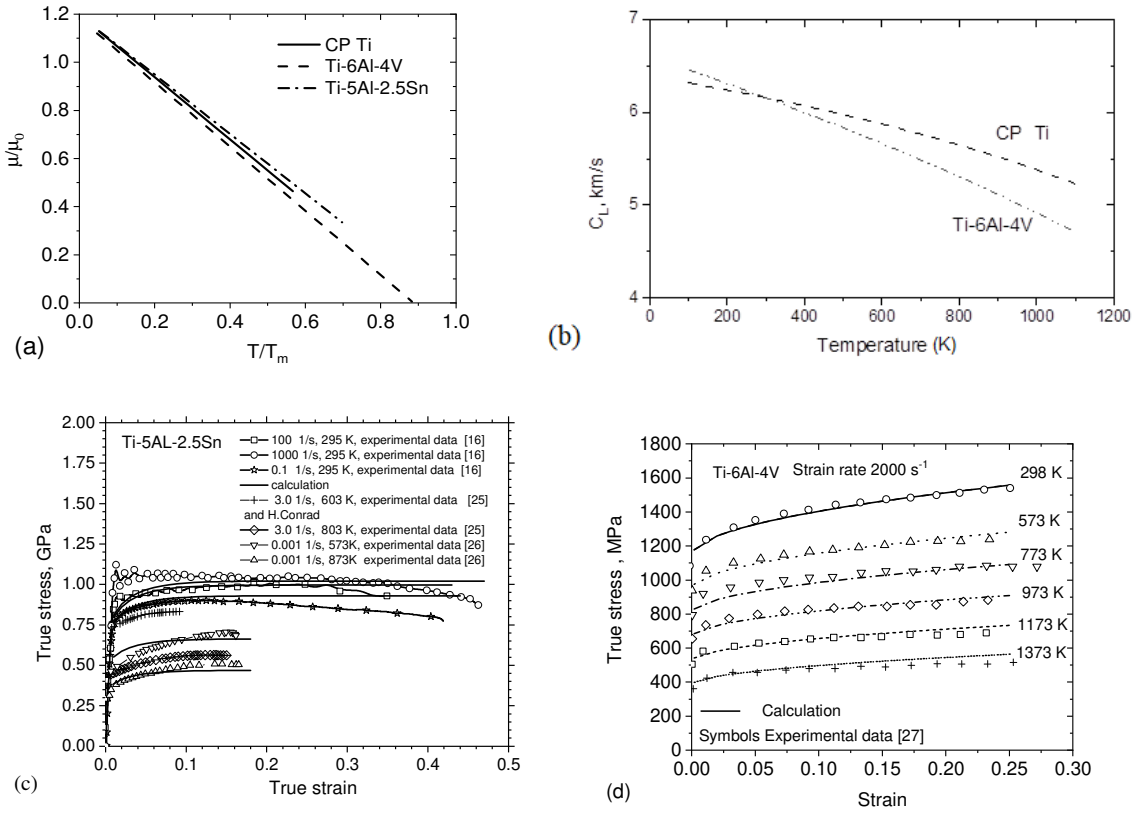

Fig.1. (a) Calculated normalized shear modulus versus homologous temperature; (b) calculated longitudinal sound velocity versus temperature; (c) calculated and experimental data of true stress versus true strain for Ti-5Al-2.5Sn; (d) the calculated true stress of Ti-6Al-4V versus logarithm of the normalized strain rates. Experimental data are shown by symbols.

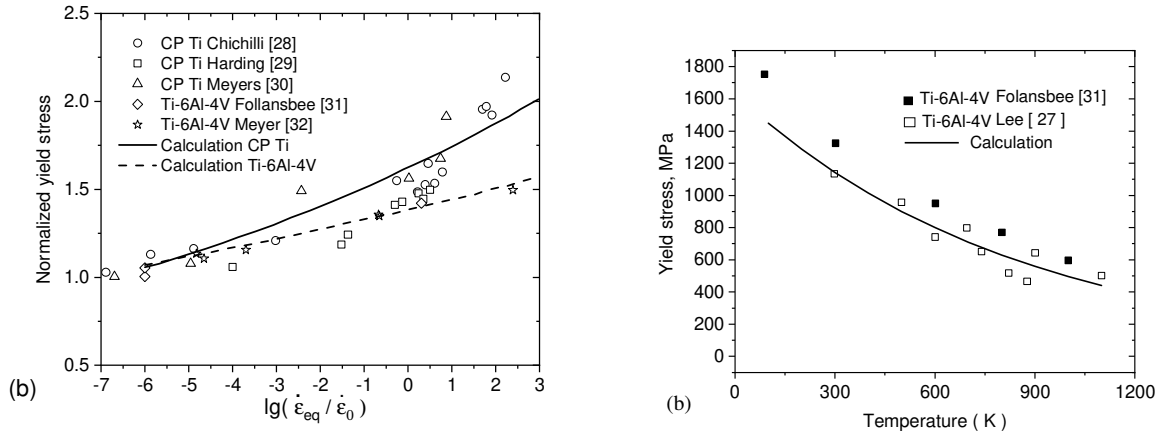

Fig.2. (a) The yield stresses of Ti-6Al-4V and CP Ti versus logarithm of the normalized strain rates. Experimental data are shown by symbols [28–32]; (b) the calculated yield stress of Ti-6Al-4V versus temperature. Experimental data are shown by symbols [27, 31].

The calculated yield stress of alpha titanium alloys versus the logarithm of the normalized strain rate is shown in Fig.2a. Experimental data [28–32] are shown by symbols. Fig.2b shows the decreasing of the calculated yield stress of Ti-6Al-4V. The simulation results are in good qualitative and quantitative agreement with the experimental data. In a wide range of strain rates and temperatures, alpha titanium alloys with different chemical compositions or microstructures demonstrate quantitative differences in changes in the values of the yield stress with the temperature and strain rate, while maintaining the regularities themselves. Thus, the simulation results showed that the yield strengths of alpha titanium alloys are structurally sensitive parameters.

Fig.3 shows the calculated free surface velocity profile of the 10 mm thick plate Ti-6Al-4V subjected to planar impact (660 m/s) by 2 mm aluminum plate versus experimental data at 295 K and 103 K, respectively. The calculated changes in the velocity of elastic precursors in Ti-6Al-4V plates are consistent with the experimental data at the specified initial temperatures. The calculation results showed that the damage growth rate increases in the spall zone with a decrease in the initial temperature. Spall fracture remains ductile in the considered temperature range, but a slight decrease in the effective spall strength is observed. The calculation results obtained agree with the experimental data [33].

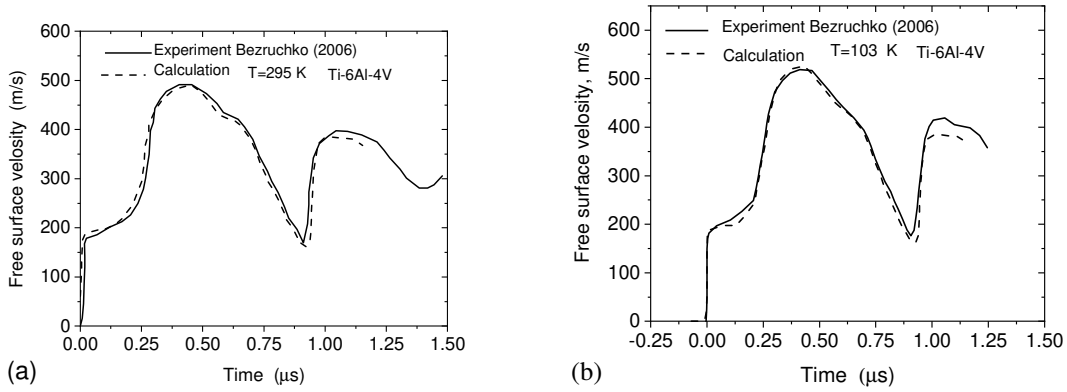

Fig.3. (a) Calculated and experimental shock wave profiles in Ti-6Al-4V at the temperature of 295 K [33]; (b) calculated and experimental [33] shock wave profiles in Ti-6Al-4V at the temperature of 103 K.

Good agreement between the calculated profiles of shock pulses including the region of unloading waves and the formation of spall fracture indicates the similarity in the mechanical response of HCP titanium alloys in the front of shock waves with amplitudes up to 10 GPa at room and low temperatures. We note that the model did not take into account the possibility of $\alpha \rightarrow \omega$ phase transformation under shock compression. The mechanical response of alpha titanium alloys was describing in shock waves and release waves. The ductile spall fracture is a result of void nucleation, growth and coalescence under repeated action of tensile and compressive stresses in interacted waves.

The results of numerical simulation showed that the damage accumulation kinetics described by equations (12)–(13) is significant for predicting the fracture dynamics at relatively low strain rates (10^2–10^3 s^{-1}). In the case of spall fracture, the limiting damage f^* in Eq. (14) is achieved in times comparable to tens and hundreds of nanoseconds. The kinetics of damage formation in the spallation zone does not play a significant role under loading by pulses of ~μs duration. It should be expected that with a decrease in the amplitude of shock pulses and an increase in the initial temperature of the loaded bodies, the kinetics of damage growth will affect the formation of dynamic fracture.

4. Conclusion

The constitutive equation for describing the mechanical behavior of alpha titanium alloys was proposed within the framework of modern physical concepts of main mechanisms providing plastic flow including the generation and sliding of dislocations, twinning and de-twinning. This constitutive equation described the mechanical response of alpha titanium alloys in a wide range of strain rates and at temperatures below the temperature of phase transition. The model's coefficients of the constitutive equation were determined using a set of data from independent experiments.

Macroscopic ductile fracture criterion can be used to predict the dynamic fracture of several alpha titanium alloys under impact of microsecond shock pulses. The use of the kinetic model of the damaged medium is justified at high strain rates (10^2–10^3 s^{-1}) under complex stress conditions, and in the spall zone and around it (10^4–10^6 s^{-1}).

The model was used for simulation of Ti-5Al-2.5 Sn and Ti-6Al-4V under uniaxial tension at strain rates from 0.1 to 1000 s^{-1}, and temperatures from 103 K to 900 K. The simulation results confirmed that strain hardening can be considered as a result of the simultaneous action of thermally activated dislocation mechanisms of plasticity and twinning, which weakly depends on temperature. The processes of spall fracture and mechanical response of titanium alloys under sub-microsecond shock pulse loading at temperatures of 103 K and 298 K at have been investigated.

The obtained results of spall fracture are consistent with the available experimental data. The calculated changes in the velocity of elastic precursors in Ti-6Al-4V plates good correlated with the experimental data at the specified initial temperatures. The calculation results showed that the damage growth rate increases in the spall zone with a decrease in the initial temperature.

The proposed model can be used to predict damage to titanium structural elements of aerospace engineering, including fan blades in the jet gas turbine engines, during high-velocity impacts of compact bodies and shock wave loading.

Acknowledgements

This work was financially supported by the Russian Science Foundation (project No. 22-79-00162).

5. References

[1] Williams J.C., Boyer R.R., *Metals*, **10**, 705, 2020; doi: 10.3390/met10060705
[2] Escobedo J.P., et al., *Acta Mater*., **60**(11), 4379, 2012; doi: 10.1016/j.actamat.2012.05.001
[3] Xiao D., Li Y., Hu S., Cai L., *J. Mater. Sci. Technol*., **26**(10), 878, 2010; doi: 10.1016/s1005-0302(10)60140-5
[4] Skripnyak V.A., Iokhim K., Skripnyak E., Skripnyak V.V., *Facta universitatis, Series: Mechanical Engineering*, **19**(1), 91, 2021; doi: 10.22190/FUME201225014S
[5] Fortin E.V., Brown A.D., Wayne L., Peralta P.D., *Proc. of the ASME 2016 Int. Mechanical Engineering Cong. and Exp. (Phoenix, Arizona, USA: ASME) IMECE2016*, 67667, 2016; doi: 10.1115/IMECE2016-67667
[6] McDonald S.A., Cotton M., Bourne N., Millett J., Withers P.J., *AIP Conf. Proc.,* **1426***,* 1065, 2012; doi: 10.1063/1.5044817
[7] Turneaure S.J., Gupta Y.M., *Journal of Applied Physics,* **106**, 033513, 2009; doi: 10.1063/1.3187929
[8] Razorenov S.V., Kanel G.I., Utkin A.V., Bogach A.A., Burkins M., Gooch W.A., *AIP Conference Proceedings,* **505**, 415, 2000; doi: 10.1063/1.1303505
[9] Zerilli F.J., Armstrong R.W., *Journal of Applied Physics,* **61**, 1816, 1987; doi: 10.1063/1.338024

[10] Johnson G.R., Cook W.H., *Proc. of the Seventh International Symposium on Ballistics, International Ballistics Committee, Hague, Netherlands*, 541, April 1983.
[11] Nemat-Nasser S., Guo W.G, Cheng J.Y., *Acta Materialia,* **47**, 3705, 1999; doi: 10.1016/S1359-6454(99)00203-7
[12] Gao C.Y., Zhang L.C., Yan H.X., *Materials Science and Engineering* – A, **528**, 4445, 2011; doi:10.1016/j.msea.2011.02.053
[13] Song Y., Voyiadjis G.Z., *European Journal of Mechanics* – A, *Solids*, **83**, 104034, 2020; doi: 10.1016/j.euromechsol.2020.104034
[14] Skripnyak V.V., Skripnyak V.A., *Journal of Applied Physics*, **131**, 165902, 2022; doi: 10.1063/5.0085338
[15] Kanel G.I., Razorenov S.V. and Utkin A.V., *High-Pressure Shock Compression of Solids II ed Davison L., Grady D.E. and Shahinpoor M.* (New York: Springer), Chapter 1, 1, 1996; doi: 10.1007/978-1-4612-2320-7_1
[16] Skripnyak V.V., Skripnyak E.G., Skripnyak V.A., *Metals*, **10**(3), 305, 2020; doi: 10.3390/met10030305.
[17] Skripnyak V.V., Kozulyn A.A., Skripnyak V.A., *Mater. Phys. Mech.* **42**, 415, 2019; doi: 10.18720/MPM.4242019_6
[18] Skripnyak V.V., Skripnyak V.A., *Metals*, **11**, 1745, 2021; doi: 10.3390/met11111745
[19] Basak D., Overfelt R.A., Wang D., *International Journal of Thermophysics*, **24**, 1721, 2003; doi: 10.1023/B:IJOT.0000004101.88449.86.
[20] Steinberg D.J., Cochran S.G., Guinan M.W., *Journal of Applied Physics,* **51**, 1498, 1980; doi: 10.1063/1.327799
[21] Souvatzis P., Eriksson O., Katsnelson M.I., *Physical Review Letters*, **99**, 015901, 2007; doi: 10.1103/PhysRevLett.99.015901
[22] ASM Ready Reference: *Thermal Properties of Metals. Hardcover*, Product code: 06702G, url: https://www.asminternational.org/home/-/journal_content/56/10192/06702G/PUBLICATION
[23] Neilsen K.L., Tvergaard V., *Eng. Fract. Mech.*, **77**, 1031, 2010; doi: 10.1016/j.engfracmech.2010.02.031
[24] Bai Y., Wierzbicki T., *International Journal of Plasticity*, **24**, 1071, 2008; doi: 10.1016/j.ijplas.2007.09.004
[25] Döner M., Conrad H., *Metall. Trans. A,* **6**, 853, 1975; doi: 10.1007/BF02672308
[26] Zhang B., Wang J., Wang Y., Li Z., Wang Y., *Mater. High Temper.*, **36**, 1, 2019; doi: 10.1080/09603409.2019.1638659
[27] Lee W.-S., Lin C.-F., *Materials Science and Engineering A*, **241**, 48, 1998; doi: 10.1016/S0921-5093(97)00471-1
[28] Chichili D.R., Ramesh K.T., Hemker K.J., *Acta Materialia*, **46**(3), 1025, 1998; doi: 10.1016/S1359-6454(97)00287-5
[29] Harding J., *Archives of Mechanics,* **27**(5-6), 715, 1975; https://rcin.org.pl/Content/138510/WA727_92860_P.262a-Harding-Temperature.pdf
[30] Meyers M.A., Subharash G., Kad B.K., Prasad L., *Mechanics of Materials*, **17**, 175, 1994; doi: 10.1016/0167-6636(94)90058-2
[31] Follansbee P.S., Gray G.T., *Metallurgical Transactions A*, **20**(5), 1989; doi: 10.1007/BF02651653
[32] Meyer L.W., Krüger L., Sommer K., Halle T., Hockauf M., *Mechanics of Time-Dependent Materials*, **12**(3), 237, 2008; doi: 10.1007/s11043-008-9060-y
[33] Bezruchko G.S., *Experimental study of the effect of temperature on the thermodynamic and mechanical properties of metals and alloys under shock-wave loading.* (PhD Thesis, Chernogolovka, 2006). (In Russian).